analytical chemistry

Article

pubs.acs.org/ac

Correlation of Carotenoid Accumulation with Aggregation and Biofilm Development in *Rhodococcus* sp. SD-74

Yi-Ting Zheng,[†] Masanori Toyofuku,[‡] Nobuhiko Nomura,[‡] and Shinsuke Shigeto*[,†]

[†]Department of Applied Chemistry and Institute of Molecular Science, National Chiao Tung University, Hsinchu 30010, Taiwan

[‡]Graduate School of Life and Environmental Sciences, University of Tsukuba, Ibaraki 305-8572, Japan

Supporting Information

ABSTRACT: Aggregation of bacterial populations substantially influences their characteristic properties and functions compared with the planktonic counterpart. It is also involved in the initial stages of biofilm development. Many studies have revealed important roles of bacterial aggregation in microbial production and biodegradation. Nevertheless, mechanistic understanding of bacterial aggregation in vivo and at the molecular level is far from complete. Here, we present a noninvasive, label-free Raman microspectroscopic approach to investigate the aggregation and biofilm development of the biotechnologically important *Rhodococcus* sp. SD-74. We found that the concentration of intracellular carotenoids increases more than 3-fold within 1 week as the biofilm develops. Raman imaging experiments confirmed that the carotenoid accumulation occurs throughout the *Rhodococcus* sp. SD-74 biofilm. The correlation between the carotenoid Raman intensities and biofilm development found in the present study provides a new means for quantitative, molecular-level assessment of the level of biofilm development, which is not possible with dye staining assay or electron microscopy. Moreover, our results suggest that microbial production of carotenoids in pigmented bacteria such as *Rhodococcus* sp. SD-74 may potentially be controlled via bacterial aggregation and biofilm formation.

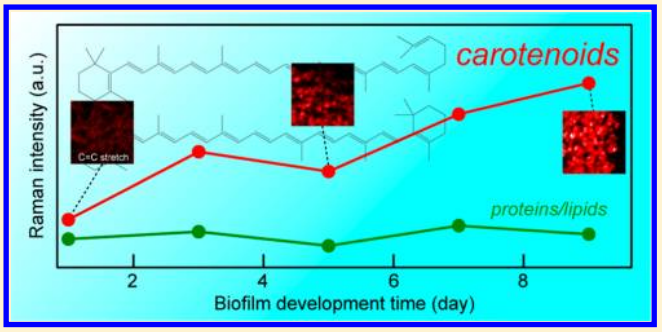

Characteristic properties and functions of bacteria are often realized and/or considerably altered when bacterial cells form aggregates rather than exist in the free-floating, planktonic state. In wastewater treatment, for example, the efficiency of the conventional activated sludge process hinges upon bioflocculation and subsequent solid−liquid separation.[1] Besides aggregates formed in culture medium, another type of bacterial aggregation can be found in biofilms, which have recently attracted keen attention because of their pivotal importance in medicine, chemical industry, and environmental science.[2−6] Biofilms are structured communities of bacterial cells that adhere to a surface or an interface, embedded in a sea of extracellular polymeric substances. Aggregation of sessile cells on a surface is involved in the initial stages of biofilm formation and dictates whether the microcolonies will evolve into a rigid biofilm structure or revert to planktonic cells.[5] If the initial aggregation can be suppressed physically or chemically, it will be possible to prevent bacterial cells from further developing hard-to-remove slime.

Despite a number of biological studies attempting to analyze bacterial aggregation, the molecular-level understanding of the underlying mechanisms remains largely unclear. To achieve this goal, we require not only molecular specificity but also space specificity, in which conventional biological approaches are lacking. Here, we present a Raman microspectroscopic approach to study the aggregation and biofilm development of the bacterium *Rhodococcus* sp. SD-74. Having nondestructive and label-free characteristics in addition to chemical and space specificities, Raman microspectroscopy and imaging offer an ideal tool for investigating microorganisms in vivo and from a molecular viewpoint.[7−13] We have recently constructed a high-sensitivity confocal Raman microspectrometer and used the developed apparatus to reveal dynamic changes in molecular concentration and distribution during the yeast cell cycle with the help of multivariate data analysis.[14] Although there has been some pioneering Raman work on biofilms relevant to wastewater treatment,[15,16] the application of Raman microspectroscopy and particularly spectral imaging[11,17] to bacterial aggregation and biofilm development is still in its infancy.

In this work, we show that the concentration of intracellular carotenoids increases substantially (more than 3-fold within 1 week) as *Rhodococcus* sp. SD-74 forms aggregates and develops biofilm. Many *Rhodococcus* strains hold promise for bioremediation because they are capable of alkane degradation,[18−20] in which bacterial aggregation has been suggested to be involved.[21] We found a positive correlation between the concentration and biofilm development only for carotenoids; other major constituents of the *Rhodococcus* sp. SD-74 biofilm,

Received: April 21, 2013
Accepted: June 26, 2013
Published: June 26, 2013

   dx.doi.org/10.1021/ac401188f | *Anal. Chem.* 2013, 85, 7295−7301

such as proteins, lipids, and nucleic acids (DNA and/or RNA), did not show such a significant variation with biofilm development. We discuss possible biological roles of the carotenoid accumulation observed in the present study. Moreover, we demonstrate that owing to intense Raman signals of carotenoids, noninvasive yet quantitative assessment of biofilm development could be achieved for pigmented bacteria by Raman microspectroscopy.

EXPERIMENTAL SECTION

Bacterial Strain and Growth Condition. *Rhodococcus* sp. SD-74, which was previously isolated from an alkaline soil sample by Uchida et al.,[22] was used in this work. This strain was precultured on a PMY agar plate at 30 °C for 1.5 days. Subsequently, it was maintained at 4 °C. PMY agar medium contained 1.0% (v/v) glycerol, 0.5% (w/v) polypepton, 0.3% yeast extract, 0.3% malt extract, 0.1% KH_2PO_4, and 1.5% agarose. The pH of the medium was adjusted to 7.0 by using KOH.

A single colony of *Rhodococcus* sp. SD-74 was harvested from the PMY agar plate and cultured in a tilted glass bottom dish containing 2 mL of tryptic soy broth as schematically shown in Figure 1. *Rhodococcus* sp. SD-74 in the tilted dish was incubated

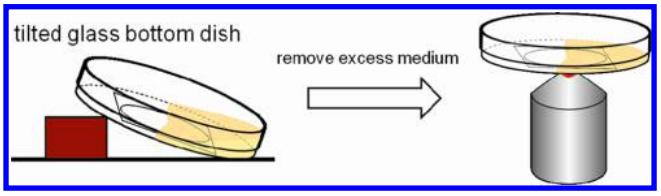

Figure 1. Scheme of the biofilm sample preparation used in the present study. *Rhodococcus* sp. SD-74 was cultured in a tilted glass bottom dish containing 2 mL of tryptic soy broth. Biofilms formed at the air−medium interface and were grown for different periods (1, 3, 5, 7, and 9 days). Excess culture broth was then gently removed from the edge of the dish by using a pipet. The resulting biofilm sample was transferred to the microscope stage for Raman measurements.

at 30 °C under high-humidity conditions, and biofilms formed at the air−medium interface. Biofilms were grown for different periods (1, 3, 5, 7, and 9 days). Before Raman spectral measurements, excess culture broth was gently removed from the edge of the dish by using a pipet, leaving only biofilm. The dish was then transferred to the microscope stage for Raman measurements. The step of removing excess culture broth was required because the glass bottom dish was eventually placed horizontally for Raman observation in an inverted microscope, as shown in Figure 1. If the medium was not removed, it would flow over the thin biofilm and break down the biofilm's structure.

Raman Microspectroscopy and Imaging. Raman spectral measurements were performed with a laboratory-built confocal Raman microscope (Figure S1, Supporting Information). Details of the apparatus were described previously.[14] In brief, the 632.8 nm output of a He−Ne laser was used as the excitation light. The beam was magnified by a factor of ∼2.7 to effectively cover the exit pupil of the objective used. The expanded beam was introduced to a custom-made inverted microscope and was focused onto the sample by an oil-immersion objective (100×, NA 1.3). The focus spot size was estimated to be about 1 μm. The laser power at the sample point was 2.6 mW throughout the present study. Backscattered Raman light was analyzed by an imaging spectrometer and detected by a back-illuminated, deep-depletion, liquid-N_2 cooled charge-coupled device (CCD) detector with 100 × 1340 pixels operating at −120 °C. A 600 grooves/mm grating was used to cover a wide spectral range (>2000 cm^{-1}) with an effective spectral resolution of 7 cm^{-1}. Lateral (XY) and axial (Z) resolution was estimated to be 0.3 and 2.4 μm, respectively. For bright-field observation, the sample was illuminated by a halogen lamp and optical images were acquired by a digital camera mounted on the microscope. In imaging experiments, the sample was translated in a raster manner by a piezoelectric nanopositioner with a 0.4 μm step in both X and Y directions (41 × 41 pixels). Spectral acquisition was synchronized with sample scanning by the computer program LabVIEW (National Instruments). The exposure time was 60 s for space-resolved measurements (Figures 2 and 3b) and 1 s per pixel for imaging experiments (Figure 4 and Figure S2, Supporting Information). As a result, scanning a 16 × 16 μm^2 (41 × 41 pixels) area required about 30 min.

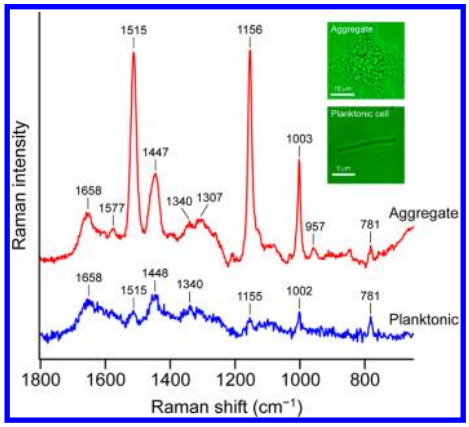

Figure 2. Raman spectra of a planktonic cell (blue) and an aggregate (red) of *Rhodococcus* sp. SD-74. The spectra were taken with excitation power of 2.6 mW at the sample point and an exposure time of 60 s. For each spectrum, the background was fitted with an eighth-order polynomial and was subtracted off (see the Experimental Section). The vertical axis applies to both planktonic and aggregate spectra, which are offset vertically for clarity of presentation. Also shown are optical images of a typical planktonic cell (lower image) and an aggregate (upper image) of *Rhodococcus* sp. SD-74. The scale bar measures 5 μm for the lower image and 10 μm for the upper image.

Data Analysis. The Raman spectrum of *Rhodococcus* sp. SD-74, regardless of planktonic cell or biofilm, typically showed high background arising mainly from the fluorescence of the medium. When analyzing Raman spectra measured with a 60 s exposure time (Figures 2 and 3b), the background in the 700−2800 cm^{-1} spectral window was fitted with an eighth-order polynomial $f(\tilde{\nu}) = \sum_{k=0}^{8} a_k \tilde{\nu}^k$ and was subtracted off from the raw data. To better determine the background, the 1800−2800 cm^{-1} region was included in polynomial fitting but is not shown in the figures below as it has no vibrational band.

To construct a Raman image, noise reduction using singular value decomposition (SVD)[7,8,14] was performed first on the fingerprint Raman spectra in the 290−2000 cm^{-1} interval (corresponding to 840 pixels). This pretreatment was needed because of low signal-to-noise ratio (S/N) in the spectra measured with a short exposure time of 1 s. The SVD was computed in IGOR Pro (WaveMetrics). The intensity of the Raman band of interest was then evaluated by calculating the

dx.doi.org/10.1021/ac401188f | Anal. Chem. 2013, 85, 7295−7301

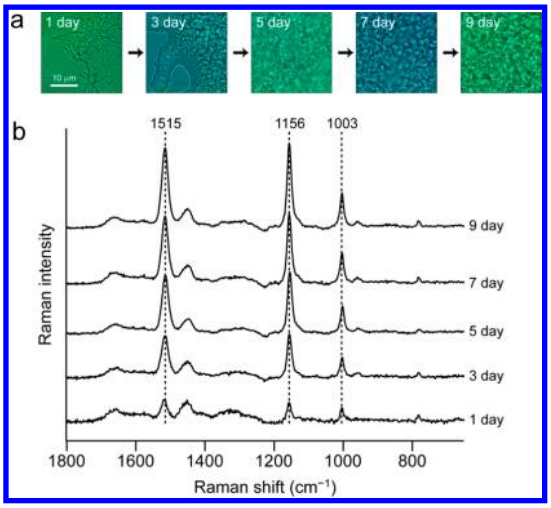

Figure 3. Carotenoid concentration increases with biofilm development in *Rhodococcus* sp. SD-74. (a) Optical images of typical *Rhodococcus* sp. SD-74 biofilms after 1, 3, 5, 7, and 9 days of growth at the air−medium interface (see Figure 1 and the Experimental Section). The scale bar in the optical images of the 1 day old biofilm measures 10 μm and applies to the other optical images as well. (b) Background-subtracted Raman spectra of 1, 3, 5, 7, and 9 day old biofilms. Each spectrum is an average of Raman spectra taken with a 60 s exposure time at randomly selected 8−10 different positions within the biofilm of a given age. The five spectra are offset vertically for clarity of presentation.

area intensity between the band contour and a baseline connecting the two ends of an interval chosen to encompass the whole band.[12] The Raman intensity thus obtained at each point was combined to construct a Raman image. Although multivariate data analysis has proven very powerful for analyzing biological Raman spectra that usually involve many overlapping contributions,[14] the univariate approach described above was effective enough in the present study because the carotenoid bands (except for the one at 1003 cm^{-1}) are nearly free from superposition of multiple Raman bands.

RESULTS AND DISCUSSION

Planktonic Cell versus Aggregate. Under static culture conditions, *Rhodococcus* sp. SD-74 represents two distinct forms, namely, planktonic form and aggregate. In planktonic form, the microorganism usually occurs as a single cell suspended in the culture medium. An optical image of typical planktonic *Rhodococcus* sp. SD-74 is shown in the lower inset of Figure 2. When cells are incubated for longer than a few days, a number of aggregates of various sizes are found on the surface of a tube used for cell culture as well as in the medium (upper inset of Figure 2). The planktonic cell and the aggregates are clearly morphologically different; the former is about 10 μm long, whereas the latter ranges from a small cluster slightly larger than a single cell, to a massive structure of hundreds of micrometers size.

Besides this morphological difference, there is a notable molecular-level difference between the two forms that is invisible by light microscopy but can be unequivocally seen by Raman microspectroscopy. The Raman spectrum in the fingerprint region (650−1800 cm^{-1}) of planktonic *Rhodococcus* sp. SD-74 (blue spectrum in Figure 2) shows vibrational bands at 1658, 1515, 1448, 1340, 1155, 1002, and 781 cm^{-1}. The band at 1658 cm^{-1} arises mainly from proteins and is assigned to the amide I mode. The bands at 1448 and 1340 cm^{-1} are both attributed to the CH bending mode of proteins and lipids, the two major intracellular components. Although lipids are a dominant component in cellular Raman spectra,[9,23,24] their contribution to the observed spectrum is probably less significant because the spectral pattern in the 1200−1400

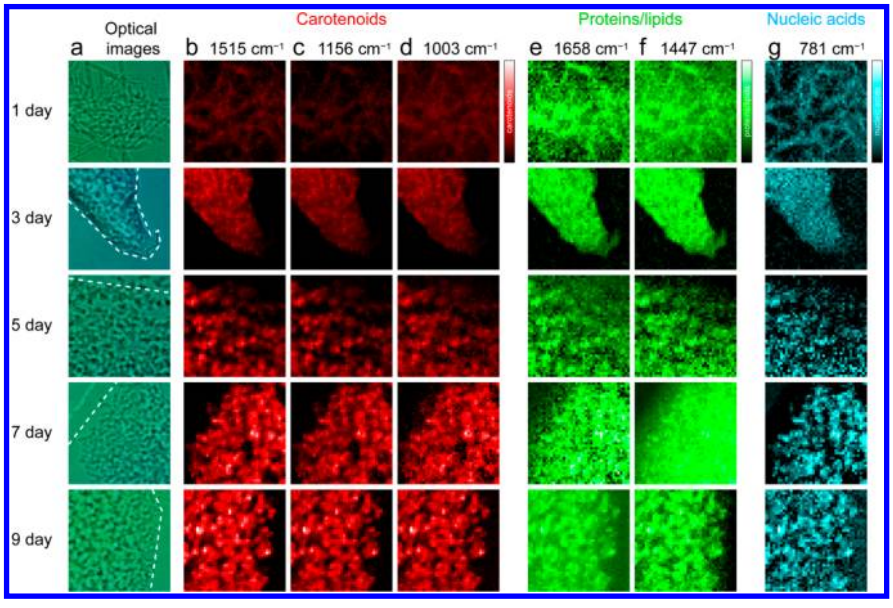

Figure 4. Multimode Raman spectral imaging of *Rhodococcus* sp. SD-74 biofilms after 1, 3, 5, 7, and 9 days of growth. (a) Optical images of the biofilms used for Raman imaging. Dashed lines in the images other than that of 1 day old define the boundary of the biofilm that is used when the average Raman intensity for each Raman image is calculated (cf. Figure 5). (b−d) Carotenoid images at the Raman shift of 1515, 1156, and 1003 cm^{-1}. (e and f) Protein/lipid Raman images at 1658 and 1447 cm^{-1}. (g) Nucleic acid Raman images at 781 cm^{-1}. The image size is 16 × 16 μm^2 (41 × 41 = 1681 pixels) for all images in panels a−g. The lowest value (corresponding to black pixels) and the highest value (white pixels) of Raman intensity used in the pseudocolor scales for panels b−g are (0, 3650), (0, 3650), (0, 930), (0, 400), (0, 570), and (0, 130), respectively. The same color scale applies to the Raman images in each column (i.e., each wavenumber).

dx.doi.org/10.1021/ac401188f | *Anal. Chem.* 2013, 85, 7295−7301

cm^{-1} region is indicative of abundant proteins, which lack the intense in-plane CH twisting band of lipids at ~1300 cm^{-1}. The band at 781 cm^{-1} is assigned to a phosphate mode of DNA/RNA plus probable contribution of a cytosine mode.[25] The remaining three weak Raman bands at 1515, 1155, and 1002 cm^{-1} are characteristic of carotenoids. They are assigned to the C═C stretching, C−C stretching, and C−CH_3 rocking modes, respectively. Due to (pre)resonance enhancement, these carotenoid Raman bands are as intense as those of abundant proteins even if carotenoids are present at a low concentration. Note that the ring-breathing mode of the phenylalanine residues of proteins may overlap with the 1002 cm^{-1} band.

It is not surprising that we observed carotenoid bands in the planktonic Raman spectrum, because a suspension of *Rhodococcus* sp. SD-74 cells is orange-colored. In fact, there have been many reports on carotenoids in other species of the *Rhodococcus* genus.[26−28] What is surprising is that those carotenoid bands are much more intense in the aggregate spectrum (red spectrum in Figure 2). The protein and nucleic acid bands at 1658, 1340, and 781 cm^{-1} are of similar intensity to those in the planktonic spectrum, whereas the three carotenoid bands are enhanced to a great extent in the aggregate spectrum. Furthermore, a weak Raman band can now be identified at 957 cm^{-1}, which is known to also arise from carotenoids. According to the normal mode calculation of β-carotene, this band is assigned to the CH out-of-plane wagging[29] and is sensitive to the conformation of the conjugated C═C bonds in carotenoids[30] (see below). We mention in passing that the weak Raman band at 1577 cm^{-1} is assigned to vibrational modes of nucleobases adenine and guanine.[24,25]

Carotenoid Concentration Increases with Biofilm Development. While measuring numerous aggregates of *Rhodococcus* sp. SD-74 in different lots of cultures, we noticed that aggregates in older culture tend to exhibit stronger carotenoid Raman bands. To test whether the intensities of the carotenoid bands positively correlate with aggregate formation, we grew *Rhodococcus* sp. SD-74 biofilms at the air−liquid interface under static conditions for 1, 3, 5, 7, and 9 days (see Figure 1 and the Experimental Section for details) and performed space-resolved Raman measurements on those biofilms of the five different ages. Representative optical images of *Rhodococcus* sp. SD-74 biofilms after 1, 3, 5, 7, and 9 days of growth show that the bacterial cells were more and more densely gathered as the biofilm development time increased (Figure 3a). Because our Raman measurements required removing excess growth medium from the sample, we were unable to trace the growth of one particular biofilm continuously over 9 days. Instead, we prepared those samples in a parallel manner so that we could do Raman measurements on all the biofilms of different ages at one time. This method allowed us to lessen the adverse effects on spectral acquisition that could be caused by possible changes in experimental conditions (e.g., focus drift and laser power drop) during a long time-lapse measurement. In most 1 day old biofilms, individual cells were distinguishable, but the older biofilms were so congested that they just looked like a rugged surface.

Figure 3b displays space-resolved Raman spectra of the *Rhodococcus* sp. SD-74 biofilms, each of which is an average of background-subtracted spectra recorded at 8−10 different positions within the biofilm of a given age. A sufficiently long exposure time of 60 s was used to achieve high S/N. The five spectra show virtually the same pattern irrespective of the age, indicating that there was no significant change in chemical composition of the biofilm. In contrast, the intensities of the carotenoid Raman bands at 1515, 1156, and 1003 cm^{-1} were indeed enhanced markedly with biofilm development. Furthermore, consistent with the data in Figure 2, little growth-time dependence was observed for the Raman bands of proteins/lipids and nucleic acids. Similar results were obtained across the biofilm thickness. We thus conclude that carotenoids, and only carotenoids, are accumulated within *Rhodococcus* sp. SD-74 cells as the biofilm develops. One may argue that the present observation could be accounted for by simply assuming an increase in cellular density in the biofilm (i.e., the amount of biomass), rather than an increase in intracellular carotenoid concentration. This argument is unlikely because the protein/lipid bands remained unchanged. Given that carotenoids (carotenes and xanthophylls) are lipophilic, it seems fairly reasonable that the carotenoids we detected mainly exist intracellularly (e.g., in lipid droplets or in the vicinity of the plasma membrane[31]). With our Raman measurements alone, however, we cannot fully rule out the possibility of extracellular carotenoids around hydrophobic *Rhodococcus* cells due to the aliphatic chains of mycolic acids in the cell wall.[18]

Carotenoid Accumulation Occurs Widespread in the Biofilm. Next, we asked whether the observed carotenoid accumulation occurs locally or nonlocally in the biofilm. This is an important question to ask, because bacterial biofilms are usually heterogeneous and the Raman spectra measured at several locations (Figure 3b) may happen to fail to grasp the whole picture of *Rhodococcus* sp. SD-74 biofilm. To answer the above question, we carried out Raman spectral imaging experiments on *Rhodococcus* sp. SD-74 biofilms after 1, 3, 5, 7, and 9 days of growth. Figure 4 shows multimode Raman images of carotenoid (1515, 1156, and 1003 cm^{-1}; Figure 4b−d), protein/lipid (1658 and 1447 cm^{-1}; Figure 4, parts e and f), and nucleic acid bands (781 cm^{-1}; Figure 4g), together with the optical images (Figure 4a). The 1658 and 1447 cm^{-1} bands cannot be unambiguously attributed to either proteins or lipids, so we use the notation protein/lipid. Because the intensity of a Raman-active mode is proportional to the concentration of the molecular species that gives rise to the mode, the Raman image represents a concentration map of the molecular species. All the six Raman images at a given biofilm development time were obtained simultaneously from one two-dimensional scan of the corresponding biofilm, which took about 30 min. Each Raman image is represented in a pseudocolor scale (red for carotenoids, green for proteins/lipids, and cyan for nucleic acids). In a red pseudocolor scale, for example, the highest Raman intensity appears white, the moderate red, and the lowest black. To facilitate comparison, we adopt different color scales for Raman images at different wavenumbers.

The Raman images classified into the three groups (Figure 4b−d, Figure 4, parts e and f, and Figure 4g) agree very well with the results of the space-resolved measurements (Figure 3b). Namely, the carotenoid concentration markedly increases as the biofilm grows for a longer period, but those of proteins and nucleic acids do not change as much. Proteins (and lipids) were abundant even after 1 day of culture. More importantly, although there are several sites that give extremely strong carotenoid signals (e.g., white spots in the Raman images of 7 day old and 9 day old biofilms), carotenoid accumulation appears to occur widespread in the entire biofilm without formation of noticeable "carotenoid pools". We repeated a similar Raman imaging experiment using a different set of

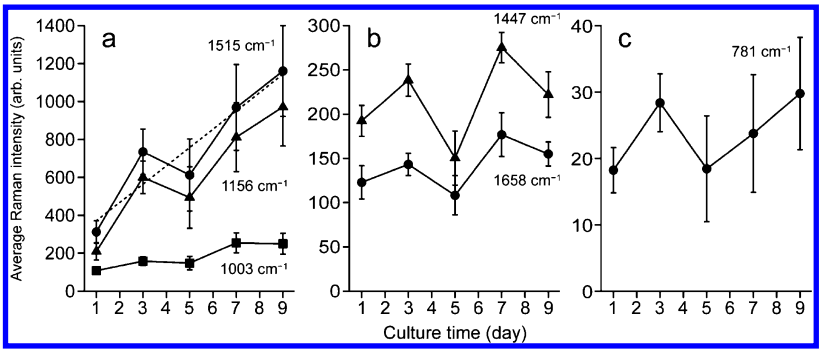

Figure 5. Culture-time dependence of the average Raman intensity for (a) the carotenoid bands, (b) protein/lipid bands, and (c) nucleic acid band, derived from the multimode Raman images of *Rhodococcus* sp. SD-74 biofilm shown in Figure 4. At each culture time, the Raman intensity of a given band in the ROI is summed up and subsequently the sum is divided by the total number of the ROI pixels (1681 pixels for the 1 day old biofilm, 835 for 3 days old, 1388 for 5 days old, 1443 for 7 days old, and 1416 for 9 days old). ROI has been defined by the dashed lines in Figure 4a. Data represent mean values ± standard deviations. The dashed line in panel a is the best fit to the time dependence of the 1515 cm^{-1} band obtained with a linear function.

Rhodococcus sp. SD-74 biofilms grown for 1, 3, and 5 days (Figure S2, Supporting Information), which verifies reproducibility of our measurements.

Quantitative Analysis of Carotenoid Accumulation. Quantitatively, how do the Raman intensities of the three major components vary with culture time? The simplest way to extract quantitative information from each Raman image is to sum up the Raman intensity in the region of interest (ROI) determined on the basis of the optical image, followed by dividing this total intensity by the number of the ROI pixels.[12] Figure 5 plots the resulting average Raman intensity as a function of culture time. The average intensities of the 1515 and 1156 cm^{-1} bands of carotenoids (Figure 5a, circles and triangles) increase almost linearly with culture time by a factor of 3.7 and 4.6, respectively, in going from 1 day to 9 days. The 1003 cm^{-1} band intensity (Figure 5a, squares) also grows but with a somewhat slower rate (about 2.3-fold increase after 9 days of growth), probably due to non-negligible contribution of the protein band (ring-breathing mode of the phenylalanine residues). As can be seen from Figure 5b, the 1658 and 1447 cm^{-1} bands (proteins/lipids) do not show any clear time dependence; their intensities appear to remain constant with some fluctuation around the mean value. The time evolution of the nucleic acid band at 781 cm^{-1} (Figure 5c) resembles those of carotenoids, but the intensity increase is only comparable to the large standard deviation of the data due to the much weaker intensity of the 781 cm^{-1} band than the other bands. A fitting of the time dependence of the 1515 cm^{-1} band intensity with a linear function yields a slope of 96 (±21) arbitrary units per day and an intercept of 275 (±122) arbitrary units (see the dashed line in Figure 5a).

For future practical applications of this linear relation, two issues need to be clarified. First, we do not have a rationale for using a linear function to describe the time dependence. Second, the linear fit cannot be immediately applied to biofilm Raman data obtained with other instruments. Some of the experimental parameters that affect Raman intensities, such as laser power, signal collection efficiency, and CCD sensitivity, may vary from experiment to experiment and from instrument to instrument, making a direct comparison difficult. We can mostly resolve this problem by using intensity ratios of the carotenoid Raman bands to the 1447 cm^{-1} band (Figure 6). The intensity of the 1447 cm^{-1} band is considered to reflect the amount of biomass within the focal volume, and hence, it can

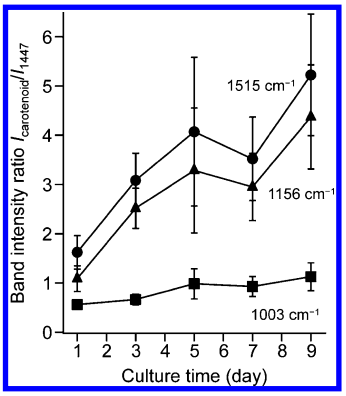

Figure 6. Culture-time dependence of the intensity ratios of the three carotenoid bands (1003, 1156, and 1515 cm^{-1}) to the 1447 cm^{-1} band. Data represent mean values ± standard deviations.

be used as an internal standard. The Raman intensity ratios of all the carotenoid bands (Figure 6) show a similar increase with biofilm development to the unnormalized Raman intensities (Figure 5a). This result reinforces our conclusion that the increase in carotenoid concentration is due to carotenoid accumulation and is not because of the presence of more bacterial cells in the probed volume. The correlation between the carotenoid Raman intensity (ratio) and biofilm development found in the present study will enable us to determine in a noninvasive yet quantitative manner the age of biofilms that consist of carotenoid-containing bacteria like *Rhodococcus* sp. SD-74, which is not possible with dye staining assay or electron microscopy.

Insight into the Chemical Identity and Structure of the Carotenoids. Vibrational spectra are often called molecular fingerprints. As such, Raman spectra not only afford chemical visualization of biomolecules in vivo, but they also provide detailed and otherwise unobtainable information on chemical identify and molecular structure. Here we focus on the observed frequency of the C═C stretching mode of carotenoids and on the occurrence of the weak band at 957 cm^{-1} in the aggregate/biofilm spectra.

The peak frequency of the C═C stretching band for all-*trans*-carotenoids has been shown to reflect the number of conjugated C═C bonds, *N*.[32] It shifts from 1508 cm^{-1} in spirilloxanthin[33] ($N = 13$), to ~1520 cm^{-1} in β-carotene[32] ($N = 11$), and to 1568 cm^{-1} in retinal[34] ($N = 5$). This dependence

dx.doi.org/10.1021/ac401188f | *Anal. Chem.* 2013, 85, 7295−7301

on the conjugated chain length can be understood by an analogy to the familiar particle in a box; the larger the length of a box, the narrower the energy level spacing between eigenstates. In *Rhodococcus* sp. SD-74, the C=C stretching band of carotenoids appears at 1515 cm^{-1}, which is indicative of carotenoids with $N \approx 11-12$. Takaichi et al. isolated four kinds of carotenoids from *Rhodococcus rhodochrous* RNMS1 and identified them using HPLC, ^1H NMR, and mass spectrometry.[26] The four carotenoid pigments all have been characterized as possessing β,ψ-carotene (γ-carotene) backbone, which contain a total of 12 C=C bonds (11 of them are conjugated). Tao and co-workers also reported that the relative species *Rhodococcus erythropolis* produces 4-keto-γ-carotene and γ-carotene.[27,28] Although we have yet to identify exactly what carotenoid pigments are present in our bacterium, we have been able to predict the polyene chain length of the carotenoids in vivo without resort to destructive chemical extraction.

A previous resonance Raman study of carotenoids in light-harvesting systems of photosynthetic bacteria including *Chromatium vinosum* and *Rhodopseudomonas palustris* showed that the relative intensity of the Raman band at ~960 cm^{-1} is sensitive to the conformations of all-*trans*-carotenoids.[30] For the planar all-trans form of a carotenoid, the 960 cm^{-1} band is very weak and appears as a shoulder of the proximate 1003 cm^{-1} band. However, when the polyene chain is distorted from the planar structure, the 960 cm^{-1} band is enhanced and exhibits a clearly discernible peak, as seen in the Raman spectra of *Rhodococcus* sp. SD-74 biofilms (Figure 3b). Thus, it is plausible that the carotenoids accumulated in *Rhodococcus* sp. SD-74 biofilms have a slightly nonplanar structure of the polyene chain, reflecting the microscopic environment of the carotenoids in the biofilm. It should be noted that the conformation we discuss here is the one in vivo; such information can never be obtained with biochemical methods.

Possible Biological Role of the Carotenoid Accumulation in *Rhodococcus* sp. SD-74. The most important challenge that the present study poses is the biological role of the carotenoid accumulation in *Rhodococcus* sp. SD-74 aggregates. Carotenoids are the most common, naturally occurring pigments found in all photosynthetic organisms (photosynthetic bacteria, microalgae, etc.) and several actinomycetes and yeasts. In microorganisms, they have been known to play a crucial role as structural components for photosystem assembly, ultraviolet (UV) screening agent, and antioxidants. Moreover, dietary carotenoids have attracted general attention because there is growing evidence from epidemiological research that they prevent many health menaces including age-related macular degeneration[35] and cancer.[36,37]

Microorganisms are thought to accumulate carotenoids as a stress response to various environmental conditions and stimuli.[38] The environmental stresses that have been discussed so far include intense UV irradiation, high temperature, and the presence of reactive oxygen species (ROS). For example, the unicellular alga *Dunaliella salina* can accumulate a huge amount of β-carotene inside the cell (up to ~10% of the dry algal biomass) when subject to the above-mentioned extreme environmental stresses.[31] A very recent study showed that *Cronobacter sakazakii*, an opportunistic food-borne pathogen, accumulates a high concentration of carotenoids in biofilms.[39] What then is the biological role of the carotenoid accumulation found in our *Rhodococcus* sp. SD-74 biofilms? First of all, the carotenoid accumulation should have nothing to do with photosynthetic functions because *Rhodococcus* sp. SD-74 is a nonphotosynthetic bacterium. Second, it is unlikely that carotenoids serve as a quencher of UV light under the present experimental conditions where the biofilm sample was not exposed to strong UV light. In our view, the antioxidant ability of carotenoids is a more plausible scenario for the present finding. As *Rhodococcus* sp. SD-74 biofilm develops, more oxidative stress would be induced in individual cells in the community due to an increase in the level of ROS. To counter the increasing oxidative stress, *Rhodococcus* sp. SD-74 cells would produce and accumulate more carotenoids. This scenario, though only speculative at present, seems consistent with work done by Boles and Singh, which showed that endogenous oxidative stress is central to produce diversity in *Pseudomonas aeruginosa* biofilms.[40]

CONCLUSIONS

In this work, we have applied noninvasive, label-free Raman microspectroscopy and imaging to *Rhodococcus* sp. SD-74 biofilms and have revealed that, compared to planktonic form, the intracellular concentration of carotenoids in the biofilm increases substantially as the biofilm develops (up to 9 days of culture). Although several earlier Raman studies did observe accumulation of carotenoids in microcolonies[41] and in biofilms,[16,39] the present study is the first, to our knowledge, to link carotenoid accumulation in biofilms directly to biofilm development. This link may lead to applications in applied microbiology and biotechnology, because it suggests that microbial production of carotenoids could be enhanced by appropriately controlling the formation of aggregates and biofilms. Raman microspectroscopy and imaging should be applicable to aggregates and biofilms of any kinds of pigmented microorganisms. Employing shorter wavelength (e.g., 532 nm) excitation will allow us to further reduce data acquisition time owing to greater resonance Raman enhancement. Thus, comprehensive Raman investigations are sure to make significant contribution to this issue.

ASSOCIATED CONTENT

Supporting Information

Additional information as noted in text. This material is available free of charge via the Internet at http://pubs.acs.org.

AUTHOR INFORMATION

Corresponding Author

*E-mail: shigeto@mail.nctu.edu.tw.

Notes

The authors declare no competing financial interest.

ACKNOWLEDGMENTS

This work was supported by the "Aiming for the Top University" plan of National Chiao Tung University. S.S. is grateful for support from the National Science Council of Taiwan Grants NSC100-2113-M-009-009-MY2 and NSC100-2738-M-009-002.

REFERENCES

(1) Busch, P. L.; Stumm, W. *Environ. Sci. Technol.* **1968**, *2*, 49−53.
(2) Costerton, J. W.; Lewandowski, Z.; Caldwell, D. E.; Korber, D. R.; Lappin-Scott, H. M. *Annu. Rev. Microbiol.* **1995**, *49*, 711−745.
(3) Davies, D. *Nat. Rev. Drug Discovery* **2003**, *2*, 114−122.
(4) Stewart, P. S.; Franklin, M. *Nat. Rev. Microbiol.* **2008**, *6*, 199−210.
(5) Monds, R. D.; O'Toole, G. A. *Trends Microbiol.* **2009**, *17*, 73−87.
(6) Joo, H.-S.; Otto, M. *Chem. Biol.* **2012**, *19*, 1503−1513.

(7) Uzunbajakava, N.; Lenferink, A.; Kraan, Y.; Volokhina, E.; Vrensen, G.; Greve, J.; Otto, C. *Biophys. J.* **2003**, *84*, 3968−3981.
(8) van Manen, H.-J.; Kraan, Y. M.; Roos, D.; Otto, C. *J. Phys. Chem. B* **2004**, *108*, 18762−18771.
(9) Huang, Y.-S.; Karashima, T.; Yamamoto, M.; Hamaguchi, H. *Biochemistry* **2005**, *44*, 10009−10019.
(10) Matthäus, C.; Boydston-White, S.; Miljković, M.; Romeo, M.; Diem, M. *Appl. Spectrosc.* **2006**, *60*, 1−8.
(11) Noothalapati Venkata, H. N.; Nomura, N.; Shigeto, S. *J. Raman Spectrosc.* **2011**, *42*, 1931−1915.
(12) Huang, C.-K.; Hamaguchi, H.; Shigeto, S. *Chem. Commun.* **2011**, *47*, 9423−9425.
(13) Okada, M.; Smith, N. I.; Palonpon, A. F.; Endo, H.; Kawata, S.; Sodeoka, M.; Fujita, K. *Proc. Natl. Acad. Sci. U.S.A.* **2012**, *109*, 28−32.
(14) Huang, C.-K.; Ando, M.; Hamaguchi, H.; Shigeto, S. *Anal. Chem.* **2012**, *84*, 5661−5668.
(15) Sandt, C.; Smith-Palmer, T.; Pink, J.; Brennan, L.; Pink, D. *J. Appl. Microbiol.* **2007**, *103*, 1808−1820.
(16) Wagner, M.; Ivleva, N. P.; Haisch, C.; Niessner, R.; Horn, H. *Water Res.* **2009**, *43*, 63−76.
(17) Ivleva, N. P.; Wagner, M.; Szkola, A.; Horn, H.; Niessner, R.; Haisch, C. *J. Phys. Chem. B* **2010**, *114*, 10184−10194.
(18) Bell, K. S.; Philp, J. C.; Aw, D. W. J.; Christofi, N. *J. Appl. Microbiol.* **1998**, *85*, 195−210.
(19) van Beilen, J. B.; Smits, T. H. M.; Whyte, L. G.; Schorcht, S.; Röthlisberger, M.; Plaggemeiser, T.; Engesser, K.-H.; Witholt, B. *Environ. Microbiol.* **2002**, *4*, 676−682.
(20) Wentzel, A.; Ellingsen, T. E.; Kotlar, H.-K.; Zotchev, S. B.; Throne-Holst, M. *Appl. Microbiol. Biotechnol.* **2007**, *76*, 1209−1221.
(21) Bouchez-Naïtali, M.; Blanchet, D.; Bardin, V.; Vandecasteele, J.-P. *Microbiology* **2001**, *147*, 2537−2543.
(22) Uchida, Y.; Tsuchiya, R.; Chino, M.; Hirano, J.; Tabuchi, T. *Agric. Biol. Chem.* **1989**, *53*, 757−763.
(23) Maquelin, K.; Kirschner, C.; Choo-Smith, L.-P.; Braak, N. v. d.; Endtz, H. P.; Naumann, D.; Puppels, G. J. *J. Microbiol. Methods* **2002**, *51*, 255−271.
(24) Naumann, D. *Appl. Spectrosc. Rev.* **2001**, *36*, 239−298.
(25) Carey, P. R. *Biochemical Applications of Raman and Resonance Raman Spectroscopies*; Academic Press: New York, 1982.
(26) Takaichi, S.; Ishidsu, J.; Seki, T.; Fukuda, S. *Agric. Biol. Chem.* **1990**, *54*, 1931−1937.
(27) Tao, L.; Cheng, Q. *Mol. Genet. Genomics* **2004**, *272*, 530−537.
(28) Tao, L.; Winona Wagner, L.; Rouvière, P. E.; Cheng, Q. *Appl. Microbiol. Biotechnol.* **2006**, *70*, 222−228.
(29) Saito, S.; Tasumi, M. *J. Raman Spectrosc.* **1983**, *14*, 310−321.
(30) Iwata, K.; Hayashi, H.; Tasumi, M. *Biochim. Biophys. Acta* **1985**, *810*, 269−273.
(31) Lamers, P. P.; Janssen, M.; De Vos, R. C. H.; Bino, R. J.; Wijffels, R. H. *Trends Biotechnol.* **2008**, *26*, 631−638.
(32) Withnall, R.; Chowdhry, B. Z.; Silver, J.; Edwards, H. G. M.; de Oliveira, L. F. C. *Spectrochim. Acta* **2003**, *A59*, 2207−2212.
(33) Okamoto, H.; Sekimoto, Y.; Tasumi, M. *Spectrochim. Acta* **1994**, *A50*, 1467−1473.
(34) Cokingham, R. E.; Lewis, A.; Collins, D. W.; Marcus, M. A. *J. Am. Chem. Soc.* **1976**, *98*, 2759−2763.
(35) Seddon, J. M.; Ajani, U. A.; Sperduto, R. D.; Hiller, R.; Blair, N.; Burton, T. C.; Farber, M. D.; Gragoudas, E. S.; Haller, J.; Miller, D. T.; Yannuzzi, L. A.; Willett, W. *JAMA, J. Am. Med. Assoc.* **1994**, *272*, 1413−1420.
(36) Männistö, S.; Smith-Warner, S. A.; Spiegelman, D.; Albanes, D.; Anderson, K.; van den Brandt, P. A.; Cerhan, J. R.; Colditz, G.; Feskanich, D.; Freudenheim, J. L.; Giovannucci, E.; Goldbohm, R. A.; Graham, S.; Miller, A. B.; Rohan, T. E.; Virtamo, J.; Willett, W. C.; Hunter, D. J. *Cancer Epidemiol., Biomarkers Prev.* **2004**, *13*, 40−48.
(37) Peto, R.; Doll, R.; Buckley, J. D.; Sporn, M. B. *Nature* **1981**, *290*, 201−208.
(38) Bhosale, P. *Appl. Microbiol. Biotechnol.* **2004**, *63*, 351−361.
(39) Du, X.-j.; Wang, F.; Lu, X.; Rasco, B. A.; Wang, S. *Res. Microbiol.* **2012**, *163*, 448−456.
(40) Boles, B. R.; Singh, P. K. *Proc. Natl. Acad. Sci. U.S.A.* **2008**, *105*, 12503−12508.
(41) Goodwin, J. R.; Hafner, L. M.; Fredericks, P. M. *J. Raman Spectrosc.* **2006**, *37*, 932−936.